Herterich, J., Black, L., Richardson, I.

Microstructure and Phase Assemblage of Low-Clinker Cements during Early Stages of Carbonation

1. Introduction

It is well established that a reduced rate of hydration is observed in composite cement materials, but there remains a lack of knowledge regarding the early age reaction kinetics of the separate phases. This may become important when considering early removal of formwork in practice. Furthermore, the reduced $Ca(OH)_2$ content, characteristic of composite cements, presents additional limitations when considering resistance to carbonation induced corrosion. The decrease in portlandite content results in a reduced pH; allowing carbonation to progress more readily. This behaviour is likely to become more pronounced with increasing levels of replacement. Moreover, the expected retardation of the rate of CO_2 ingress typically observed in PC systems upon carbonation is a result of densification of the microstructure. This, however, is not concurrent with the behaviour exhibited in composite cements with high replacement levels, in which carbonation may lead to a coarser microstructure and greater porosity.
This study investigates the effects of carbonation following short curing periods (72 h) on CEMI and composite cement systems (30% PFA & 30% GGBS). Carbonation behaviour changed compared to 'idealised'/28 day lab cured samples and accelerated carbonation testing. Carbonation of $Ca(OH)_2$ and C-S-H did not occur simultaneously, with decalcification of C-S-H only beginning once no more $Ca(OH)_2$ was available. Decalcification and dealumination of the C-S-H phase occurred following exposure to ambient [CO_2], and $CaCO_3$ microcrystals were observed in the outer product (Op) regions only. A reduction in the Ca/Si ratio of the Ip C-S-H appears to be a result of migration of the Ca ions, driven by a concentration gradient. Furthermore, the rate and extent of carbonation and the nature of the carbonate species formed is dependent on both the level of replacement and the replacement material.

2. Experimental program

2.1. Raw Materials

A CEM I 52.5R cement was selected for this study; to ensure early age strength development in the composite systems. The chemical composition, determined by x-ray fluorescence (XRF), for the CEM I 52.5R, PFA and GGBS used are shown in Table 1. Table 2 displays the mineralogical composition of the cement clinker.

Table 1:
Chemical composition of raw materials

		LOI	SiO_2	Al_2O_3	Fe_2O_3	TiO_2	MnO	CaO	MgO	SO_3	K_2O	Na_2O	P_2O_5	Total
CEM I 52.5R	%	1.50	20.50	4.60	2.40	0.30	0.00	63.40	2.00	3.60	0.74	0.13	0.30	99.47
PFA	%		70.83	24.36	2.24	1.48	0.05	0.06	0.23	0.00	0.64	0.10	0.05	100.04
GGBS	%	2.35	35.71	10.65	0.45	0.73	0.23	43.32	3.97	3.06	0.45	0.16	0.02	98.74

Table 2:
Mineralogical composition of CEMI 52.5R (determined by Bogue calculation)

		C_3S	C_2S	C_3A	C_4AF
CEM 52.5R	%	68	10	9	7

2.2. Experimental

Three paste systems (CEMI, and CEMI with 30% replacement by volume of PFA or GGBS), w/b = 0.57, were investigated. The CEM I used was free from limestone. Samples were cast and sealed in small plastic vials (ø = 12 mm, h = 47 mm) and rotated for 72 hours (t_0) at 22º +/-2ºC. This allowed the systems to develop enough strength to allow sample preparation and conditioning, while still replicating early removal of formwork. Samples were then sliced 0.5 mm thick; to study carbonation kinetics without impact from the effects of porosity and transport properties. Therefore, it is implied that the study characterises the carbonation behaviour of the concrete in the cover region, rather than of the bulk concrete. Cut samples were subjected to conditioning at either ambient CO_2 conditions (300-400 ppm CO_2, approx. 24ºC) or in a CO_2 free environment. All samples were conditioned at a relative humidity (RH) of 72.6% for up to 14 days. Characterisation was performed at t_0, 1, 2, 4, 7 & 14 days. All samples were hydration stopped prior to analysis by immersion in isopropanol for a period of 2 hours and then washed 3 times with diethyl ether and finally heated at 40ºC on a hotplate for 10 minutes[1].

Attenuated total reflectance (ATR) FTIR spectroscopy was performed over a wavenumber range 0 - 4000cm^{-1}. Analytical TEM data was collected on Ar ion-beam milled samples. ^{29}Si MAS NMR and ^{27}Al MAS NMR spectra were collected by the solid-state NMR service at Durham University. The ^{29}Si NMR spectra were collected at an operating frequency of 79.438MHz, a spin rate of 6000Hz and pulse duration of 4.5µs. The spectra for the GGBS system used a 20ms acquisition time and a 5.0s recycle time for 1300 repetitions. The PFA spectra were collected with a 30ms acquisition time and a 1.0s recycle time for 1400 and 2400 repetitions for the non-carbonated and carbonated samples respectively. ^{27}Al spectra were collected at an operating frequency of 104.199MHz, and spin speeds of 12000Hz for the PFA systems, 12957Hz for the non-carbonated GGBS systems and 13061Hz for the carbonated GGBS systems, and no proton decoupling. A pulse duration of 1.0µs, 10ms acquisition time and 0.2s recycle time were used for all samples. The number of repetitions were 3100 (non-carbonated GGBS), 6000 (non-carbonated PFA & carbonated GGBS) and 4350 (carbonated PFA). The ^{29}Si spectra were fitted with peaks using a Voigt line shape and the resulting data used to calculate the mean aluminosilicate chain length and mean Al/Si ratio of the samples. Deconvolutions were verified to be correct when the Al/Si ratio was in good agreement with that calculated from analytical TEM data.

3. Results and discussion

ATR-FTIR data were collected for all the samples exposed to ambient CO_2. Figure 1 displays the characteristic carbonates stretching band at 1400 - 1500cm^{-1} collected for the 30% GGBS system. Exposure to CO_2 led to progressive carbonation. However a substantial increase is observed between 2 and 4 days. Figure 2 shows the normalised spectra for the silicate bands (a) and the $Ca(OH)_2$ peak (b). The consumption of $Ca(OH)_2$ and the decalcification of C-S-H, indicated by a small shift in the silicate band to a higher wavenumber, are concurrent with the large increase in $CaCO_3$ content. The consumption of portlandite, and therefore the loss of buffering capacity, permits a more rapid rate of carbonation within the sample. Furthermore the early age carbonation of $Ca(OH)_2$ and C-S-H are not simultaneous, as widely reported for well-cured systems[2], but carbonation of C-S-H only begins once there is no more $Ca(OH)_2$ available.

Similar behaviour was seen for the 30% PFA system, whereas in the CEMI system it was observed between 4 and 7 days. The loss of buffering capacity at an earlier age in

the composite cements is a result of their lower initial $Ca(OH)_2$ contents, and is expected to occur at increasingly earlier ages with increasing levels of replacement.

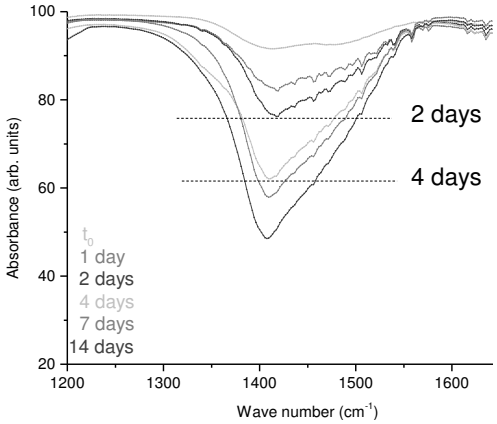

Figure 1: ATR-FTIR spectra for 30% GGBS exposed to ambient [CO_2] showing $CaCO_3$ content between 1000 – 1800cm^{-1}

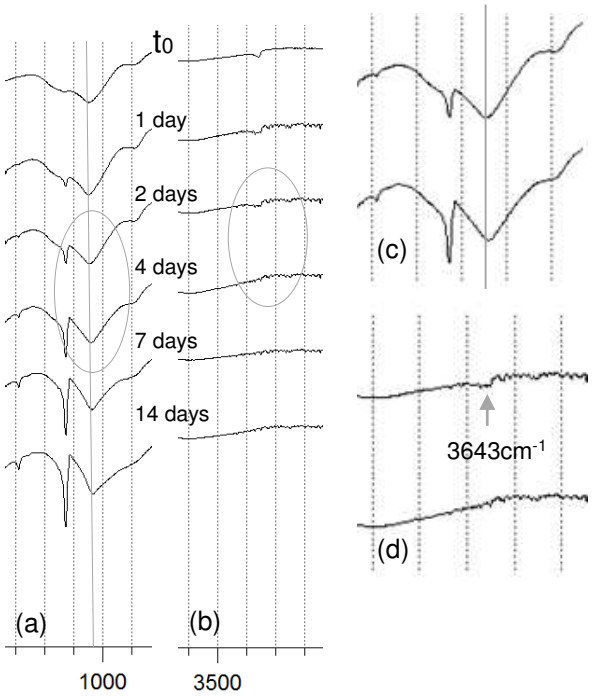

Figure 2: ATR-FTIR spectra for 30% GGBS exposed to ambient [CO_2] showing (a) silicate bands (with magnification of circled area shown (c)) and (b) $Ca(OH)_2$ peak (3643cm^{-1}) (with magnification of circled area shown in (d))

TEM-EDX analyses of both inner product (Ip) and outer product (Op) C-S-H were collected following 7 days exposure for the CEMI system and 4 days for the composite systems. All areas were free from crystalline phases. The mean Ca/Si, Ca/(Al+Si) and Al/Si ratios for Ip and Op C-S-H are given in Table 3 for the non-carbonated CEMI sample. The Ca/Si ratio of 1.70 is in good agreement with that typically recorded for neat PC systems[3]. It is interesting to note a bimodal distribution is exhibited; in agreement with [4] which showed a bimodal distribution of the Ca/Si ratio in young pastes which subsequently became unimodal with time.

Table 3:
Mean Ca/Si, Ca/(Al+Si) and Al/Si ratios for C-S-H for CEMI conditioned for 7 days at 0% [CO_2]

		Ca/Si		Ca/(Al+Si)		Al/Si	
	N	Mean	S.D.	Mean	S.D.	Mean	S.D.
Op	20	1.61	0.14	1.45	0.11	0.11	0.03
Ip	20	1.79	0.17	-	-	0.07*	-
All	40	1.70	0.18				

N = number of analyses, S.D. = standard deviation
*Determined from regression analysis of Al/Si-Mg/Si plots at Mg/Si = 0

EDX data collected for the 30% GGBS system is given in Table 4 for both the non-carbonated (4(a)) and carbonated (4(b)) samples. The sample conditioned in a CO_2 free environment had a Ca/Si ratio of 1.39 and an Al/Si ratio of 0.16 (Op) and 0.11 (Ip).

The decreased Ca/Si ratio and increased Al/Si ratio, compared to the CEMI system, is a relationship well established in the literature [5, 6]. Furthermore, the decreased Ca/Si ratio indicates considerable reaction of the slag. The Mg/Al ratio of the hydrotalcite-like phase (derived from the linear regression plot of Al/Si – Mg/Si) was determined to be 2.78 for the 0% CO_2 system; higher than the values of 2 reported for many older samples. However, the ratio is predicted to decrease with age [6]. The Ca/Si ratio for the carbonated slag sample (Ca/Si 0.57) confirms C-S-H decalcification, supporting the ATR-FTIR data. Comparing the level of carbonation of the Ip and Op regions, (calculated from the change in Ca/Si ratio before and after carbonation), both regions have undergone similar levels of decalcification; Ip = 56.6%, Op = 59.5%. This decrease in Ca/Si ratio is also accompanied by a decrease in the Al/Si ratio of the Op region, with dealumination of the C-(A)-S-H phase from an Al/Si ratio of 0.16 to 0.10. Additional EDX data points are required to accurately calculate the Al/Si ratio of the Ip C-S-H and Mg/Al of the hydrotalcite-like phase, and are therefore not shown here.

Table 4:
Mean Ca/Si, Ca/(Al+Si) and Al/Si ratios for C-S-H for 30% GGBS (as previously shown in [7])

(a) conditioned for 4 days at 0% [CO_2]

		Ca/Si		Ca/(Al+Si)		Al/Si	
	N	Mean	S.D.	Mean	S.D.	Mean	S.D.
Op	50	1.48	0.18	1.28	0.12	0.16	0.07
Ip	25	1.22	0.08	-	-	0.11*	-
All	75	1.39	0.20				

(b) conditioned for 4 days at ambient [CO_2]

		Ca/Si		Ca/(Al+Si)		Al/Si	
	N	Mean	S.D.	Mean	S.D.	Mean	S.D.
Op	15	0.60	0.07	0.55	0.06	0.10	0.03
Ip	33	0.53	0.06	-	-	-	-
All	35	0.57	0.07				

N = number of analyses, S.D. = standard deviation
*Determined from regression analysis of Al/Si-Mg/Si plots at Mg/Si = 0

Table 5(a) displays the EDX data collected for the 30% PFA sample conditioned at 0% CO_2. Following hydration for only 72 hours, minimal or no measurable reaction of PFA was expected[8,9]. However, the Ca/Si ratio for the non-carbonated sample of 1.55 (compared to 1.70 for the CEM I system) indicates slight reaction of the PFA has occurred. However, the extent of reaction is less than for the slag sample, where a Ca/Si ratio of 1.39 was observed. Girao *et al*. (2010) [10] reported Ca/Si ratios of 1.41 and 1.49 for Ip and Op regions, respectively, in a 30% PFA system hydrated for one month, emphasising the slower reaction rates typical of PFA. A slightly higher Al/Si ratio for the PFA sample, Op 0.13, compared to the neat system, Op 0.11, but a lower ratio than that of the slag system, Op 0.16, further corroborates this observation.
EDX data was collected for the carbonated PFA sample (Table 5(b)). This was more challenging for the fly ash sample, areas of C-S-H that were wholly amorphous were more difficult to find, and currently no EDX analyses were possible for Op regions. Not only does this indicate a greater extent of carbonation in the sample, but the slower reaction rate is likely to have produced a less developed, porous, microstructure, in which CO_2 is able to diffuse through more readily, and in which the availability of

hydrate phases for carbonation is lower in comparison to the slag system. Decalcification of Ip C-S-H is confirmed by the decrease in Ca/Si ratio, again verifying the results from the ATR-FTIR analysis.

Table 5:
Mean Ca/Si, Ca/(Al+Si) and Al/Si ratios for C-S-H for 30% PFA

(a) conditioned for 4 days at 0% [CO_2] (as previously shown in [7])

		Ca/Si		Ca/(Al+Si)		Al/Si	
	N	Mean	S.D.	Mean	S.D.	Mean	S.D.
Op	25	1.62	0.10	1.37	0.09	0.13	0.05
Ip	19	1.53	0.08	-	-	-	-
All	44	1.55	0.10				

(b) conditioned for 4 days at ambient [CO_2]

		Ca/Si		Ca/(Al+Si)		Al/Si	
	N	Mean	S.D.	Mean	S.D.	Mean	S.D.
Op	-	-	-	-	-	-	-
Ip	16	0.86	0.14	-	-	0.09	0.02
All	16	0.86	0.14				

N = number of analyses, S.D. = standard deviation

TEM micrographs from the GGBS and PFA samples are displayed in Figures 3 and 4 respectively. Non-carbonated and carbonated samples are shown in Figures (3, 4) (a) and (3, 4) (b) & (c) respectively. Fibrillar and foil like morphology of the Op C-S-H is evident in both systems, confirming the reduction in Ca/Si ratio already observed in the EDX data [5]. The carbonated samples in Figures 3(b) and 4(b) display a coarsening of the Op C-S-H as a result of carbonation, corresponding to decalcification of the C-S-H. Ip regions showed no change in the microstructure. Microcrystals of $CaCO_3$ were observed in the Op regions only, Figures 3(c) and 4(c), forming on fibrils of Op C-S-H. SAED patterns confirmed the microcrystals to be calcite in the GGBS cement, and both calcite and vaterite in the PFA blend. The microgrpahs indicate the Ip C-S-H has been unaffected by carbonation, however EDX data clearly shows decalcification has occurred, with a similar level observed for both Ip and Op regions in the slag system. Groves *et al* (1990) [11], proposed that the decrease in the Ca/Si ratio of the Ip C-S-H without any visual change in the microstructure was the cause of carbonation shrinkage; the Ca^{2+} cations migrating from Ip regions to Op regions in order to maintain equilibrium due to a concentration gradient.

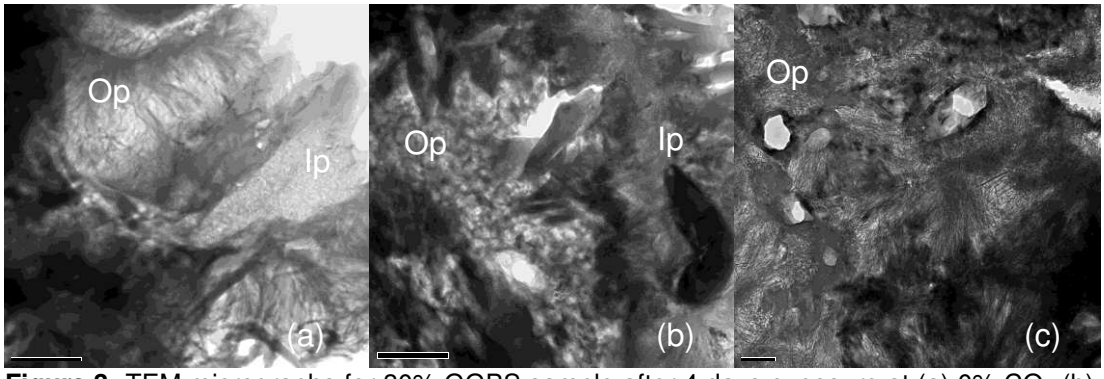

Figure 3: TEM micrographs for 30% GGBS sample after 4 days exposure at (a) 0% CO_2 (b) (as previously shown in [7]), & (c) ambient CO_2

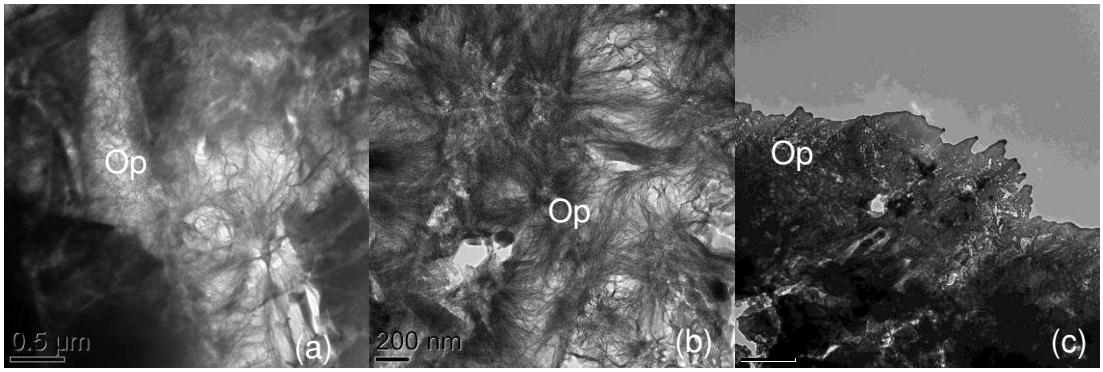

Figure 4: TEM micrographs for 30% PFA sample after 4 days exposure at (a) 0% CO_2 (b) & (c) ambient CO_2

Figure 5 shows the ^{29}Si MAS NMR spectra collected for the 30% GGBS sample, as well as the fitted hydrate peaks and fitted spectra. The results from the deconvolution of the spectra for both the slag and the PFA systems are given in Table 6. Both Figure 5 and Table 6 reveal a reduction in the intensity of the Q^1 peak (end-chain unit) as a result of carbonation for both systems. This decrease is accompanied by a large increase in the Q^2 peak (dimeric silicate unit), with a resulting increase in the mean aluminosilicate chain length (MCL). The increased polymerisation confirms the decalcification of the C-S-H phase [12]. The MCL of the two non-carbonated systems are similar, however a greater degree of polymerisation is evident in the PFA sample following exposure to CO_2. A small reduction in the intensity of the $Q^2(1Al)$ peak was also observed for the carbonated systems, this is a further indication that withdrawal of Al from the C-(A)-S-H phase has occurred, as previously observed in the TEM-EDX analysis. Consequently, both data sets see a decrease in the mean Al/Si ratio following exposure to ambient CO_2 concentrations.

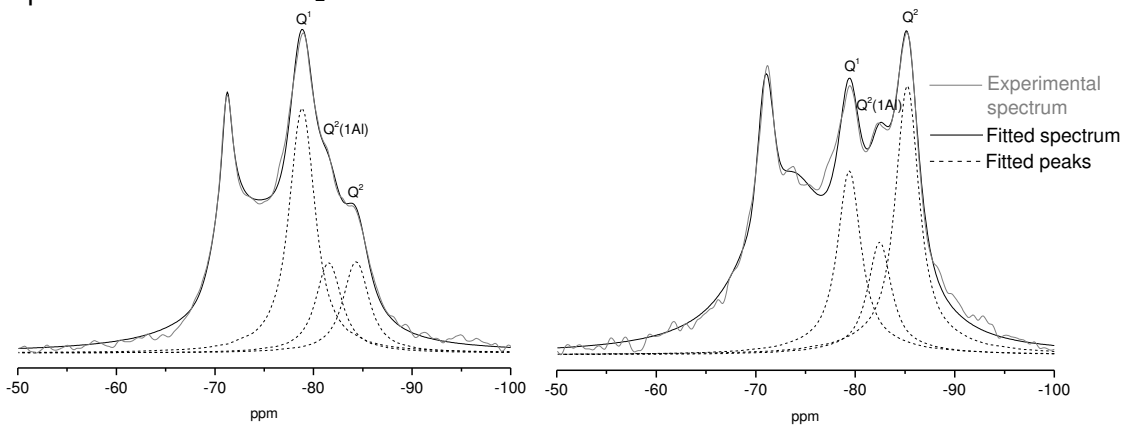

Figure 5: Single-pulse ^{29}Si MAS NMR spectra for 30% GGBS samples following 4 days exposure at (a) 0% [CO_2] (b) ambient [CO_2] (showing hydrate peak fitting only- anhydrous PC and slag peak fitting will be discussed separately from this paper)

Table 6: Results from deconvolution of Single-pulse ^{29}Si MAS NMR spectra for 30% GGBS & 30% PFA samples following 4 days exposure at 0% [CO_2] & ambient [CO_2]

		Chemical shifts (ppm)			Relative intensities (%)				Al/Si	Al/Si TEM (s.d)	
		Q^1	$Q^2(1Al)$	$Q^2(0Al)$	Q^1	$Q^2(1Al)$	$Q^2(0Al)$	MCL	Al/Si NMR	Op	Ip
30% GGBS	non-carbonated	-78.84	-81.54	-84.32	30.13	11.10	11.22	3.24	0.11	0.16 (0.07)	0.11
30% GGBS	carbonated	-79.4	-82.45	-85.23	17.29	10.55	25.07	6.73	0.10	0.10 (0.03)	-
30% PFA	non-carbonated	-78.45	-80.91	-84.5	26.34	7.14	7.81	3.41	0.09	0.13 (0.05)	0.11
30% PFA	carbonated	-78.87	-81.92	-84.98	9.5	5.88	20.47	8.16	0.08	-	-

MCL = mean aluminosilicate chain length for C-S-H

Finally, ^{27}Al MAS NMR provides some insight into the effect of carbonation on the AFm phases. Figure 6 displays the spectra collected for both the GGBS (left) and PFA (right) samples. The non-carbonated systems are shown in (a) and the carbonated systems in (b). XRD reveals no significant change in AFt content (chemical shift at ≈13ppm) at this age for the carbonated and non-carbonated samples. Following this, qualitative interpretation of the data shows a substantial decrease in the peak at ≈9ppm, in comparison to the peak attributed to AFt. Both AFm [13] and the hydrotalcite-like phase have a chemical shift at ≈9ppm, here, however, it is probable that peak is due to AFm, small amounts of AFm phases have been present in XRD data, whereas hydrotalcite has only been observed in some of the TEM analyses. Assuming the peak at ≈9ppm is due to an AFm phase, carbonation causes dramatic decomposition of this phase in both the slag and PFA sample, in which it completely disappears.

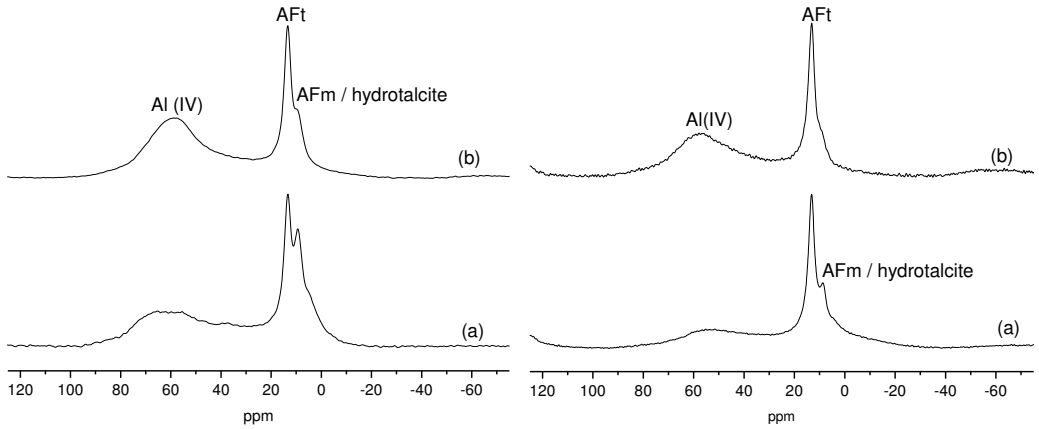

Figure 6: Single-pulse ^{27}AL MAS NMR spectra for 30% GGBS (left) & 30% PFA (right) samples following 4 days exposure at (a) 0% [CO_2] (b) ambient [CO_2]

4. Conclusions

- ATR-FTIR data showed a large increase in carbonate content following consumption of $Ca(OH)_2$, indicating carbonation is able to progress much more rapidly once portlandite, and therefore the buffering capacity, has been depleted.
- Decalcification of the C-S-H phase only began once there was no more $Ca(OH)_2$ available, unlike simultaneous carbonation of both phases as previously reported.
- TEM-EDX analyses revealed both decalcification and dealumination of the C-(A)-S-H phase in the composite materials following exposure to CO_2 for 4 days.
- TEM micrographs revealed coarsening of the Op region, with $CaCO_3$ microcrystals forming on Op C-S-H fibrils only. The decrease in Ca/Si ratio of the Ip regions was therefore attributed to the migration of Ca^{2+} cations, driven by a concentration gradient.
- ^{29}Si MAS NMR data confirmed decalcification of the C-S-H phase with a decrease in the intensity of the Q^1 peak and an increase in the intensity of the Q^2 peak following exposure to CO_2. A small reduction in the Q^2(1Al) peak further confirms the removal of Al from the C-(A)-S-H phase.
- ^{27}Al MAS NMR spectra indicate carbonation of AFm, rather than of AFt, at this age.

5. Acknowledgements
The authors thank Nanocem (nanocem.org) for funding this research and the solid-state NMR service at the University of Durham for collecting the MAS NMR spectra.

References

[1] Zhang J., Scherer G. W., 2011. Comparison of methods for arresting hydration of cement. *Cement and Concrete Research*, 41, 1024-1036.

[2] Groves, G.W., et al., 1991. *Progressive Changes in the Structure of Hardened C3S Cement Pastes due to Carbonation.* Journal of the American Ceramic Society, 74(11), 2891-2896.

[3] Richardson I. G., 2000. The nature of the hydration products in hardened cement pastes. *Cement and Concrete Composites*, 22, 97-113.

[4] Richardson I. G., Groves G. W., 1993. Microstructure and microanalysis of hardened ordinary Portland cement pastes. *Journal of Materials Science*, 28, 265-277.

[5] Richardson I. G., Groves G. W., 1992. Microstructure and microanalysis of hardened cement pastes involving ground granulated blast-furnace slag. *Journal of Materials Science*, 27, 6204-6212.

[6] Taylor R., *et al* 2010. Composition and microstructure of 20-year-old ordinary Portland cement-ground granulated blast furnace slag blends containing 0-100% slag. *Cement and Concrete Research*, 40, 971-983.

[7] Herterich J., et al 2015. Microstructure and phase assemblage of low-clinker cements during early stages of carbonation. The 14th *International Congress on the Chemistry of Cement Conference Proceedings.* 13th-16th October 2015, Beijing, China.

[8] Deschner F., *et al*, 2012. Hydration of Portland cement with high replacement by siliceous fly ash. *Cement and Concrete Research*, 42, 1389-1400.

[9] Fraay, A. L. A., *et al*, 1989. The reaction of fly ash in concrete. A critical examination. *Cement and Concrete Research*, 19, 235-246.

[10] Girao A. V., *et al*, 2010. Composition, morphology and nanostructure of C-S-H in 70% white Portland cement – 30% fly ash blends hydrated at 55^{o}C. *Cement and Concrete Research*, 40, 1350-1359.

[11] Groves G. W., *et al* 1990. The carbonation of hardened cement pastes. *Advances in Cement Research*, 3, 117-125.

[12] Sevelsted T. F., Skibsted J., 2015. Carbonation of C-S-H and C-A-S-H samples studied by ^{13}C, ^{27}Al and ^{29}Si MAS NMR spectroscopy. *Cement and Concrete Research,* 71, 56-65.

[13] Skibsted J., *et al*, 1993. Characterization of calcium aluminate phases in cemenst by 27Al MAS NMR spectroscopy. *Inorganic Chemistry*, 32, 1013-1027.

Authors:
Julia Herterich cn08j6h@leeds.ac.uk
Leon Black
Ian Richardson

Institute for Resilient Infrastructure
School of Civil Engineering
University of Leeds